Follow us @BoneJointRes

Freely available online OPEN ACCESS

BJR

INFECTION

Fracture-related infection in osteoporotic bone causes more severe infection and further delays healing

J. Li,
R. M. Y. Wong,
Y. L. Chung,
S. S. Y. Leung,
S. K-H. Chow,
M. Ip,
W-H. Cheung

From The Chinese University of Hong Kong, Hong Kong, China

Aims

With the ageing population, fragility fractures have become one of the most common conditions. The objective of this study was to investigate whether microbiological outcomes and fracture-healing in osteoporotic bone is worse than normal bone with fracture-related infection (FRI).

Methods

A total of 120 six-month-old Sprague-Dawley (SD) rats were randomized to six groups: Sham, sham + infection (Sham-Inf), sham with infection + antibiotics (Sham-Inf-A), ovariectomized (OVX), OVX + infection (OVX-Inf), and OVX + infection + antibiotics (OVX-Inf-A). Open femoral diaphysis fractures with Kirschner wire fixation were performed. *Staphylococcus aureus* at 4 × 10^4 colony-forming units (CFU)/ml was inoculated. Rats were euthanized at four and eight weeks post-surgery. Radiography, micro-CT, haematoxylin-eosin, mechanical testing, immunohistochemistry (IHC), gram staining, agar plating, crystal violet staining, and scanning electron microscopy were performed.

Results

Agar plating analysis revealed a higher bacterial load in bone (p = 0.002), and gram staining showed higher cortical bone colonization (p = 0.039) in OVX-Inf compared to Sham-Inf. OVX-Inf showed significantly increased callus area (p = 0.013), but decreased high-density bone volume (p = 0.023) compared to Sham-Inf. IHC staining showed a significantly increased expression of TNF-α in OVX-Inf compared to OVX (p = 0.049). Significantly reduced bacterial load on bone (p = 0.001), enhanced ultimate load (p = 0.001), and energy to failure were observed in Sham-Inf-A compared to Sham-Inf (p = 0.028), but not in OVX-Inf-A compared to OVX-Inf.

Conclusion

In osteoporotic bone with FRI, infection was more severe with more bone lysis and higher bacterial load, and fracture-healing was further delayed. Systemic antibiotics significantly reduced bacterial load and enhanced callus quality and strength in normal bone with FRI, but not in osteoporotic bone.

Cite this article: *Bone Joint Res* 2022;11(2):49–60.

Keywords: Fracture healing, Osteoporosis, Fracture related infection

Article focus

- It is unknown whether microbiological outcomes and fracture-healing in osteoporotic bone with fracture-related infection (FRI) are worse than normal bone with FRI.
- The therapeutic effect of systemic antibiotic treatment was assessed for decreasing bacterial load and fracture-healing.

Key messages

- Bacterial infection was more severe with increased periosteal bone formation and bone lysis in osteoporotic bone with FRI. A higher bacterial load and colonization of the osteocyte-lacuno canalicular network were present.

Correspondence should be sent to Ronald Man Yeung Wong; email: ronaldwong@ort.cuhk.edu.hk

doi: 10.1302/2046-3758.112.BJR-2021-0299.R1

Bone Joint Res 2022;11(2):49–60.

- Fracture-healing was further delayed in osteoporotic bone with FRI, which was characterized by impaired callus remodelling.
- Systemic antibiotic treatment reduced bacterial load in bone, and improved callus quality and mechanical strength in normal bone with FRI. These effects were not observed in osteoporotic bone, warranting more novel treatments.

Strength and limitations

- We are the first group to identify more severe infection and impaired healing in osteoporotic bone with FRI.
- The findings require validation in clinical studies.

Introduction

Fracture-related infection (FRI) is defined as infection that occurs after fracture fixation, and is one of the most severe complications that occur in trauma surgery.[1] Current consensus on the diagnosis of FRI is the presence of microorganisms in deep tissue specimens confirmed by histopathological examination.[1] Recent evidence has shown a rapid increase of open fractures in patients aged over 65 years.[2] With the ageing population, fragility fractures have become one of the most common problems clinicians encounter.[3,4] More importantly, 65% of wounds are often contaminated by microorganisms, of which 30% are symptomatic.[5] Clinically, FRI can lead to serious clinical consequences including nonunion, long-term antibiotic treatment, multiple debridement surgeries, long-lasting disability, and even amputation.[6,7] The average cost for treatment also ranges from USD $17,000 to $150,000 per patient,[8] leading to a significant socioeconomic burden.

It is well established that osteoporotic fracture-healing leads to impaired healing.[9-11] Interestingly, the risk of infection is also reportedly higher in cases with postmenopausal and senile osteoporosis, in which early immune response and capacity of pathogen clearance are compromised,[12] as oestrogen is suggested to be immunoprotective.[13] In fact, Gjertsson et al[14] found that mice with an ovariectomy showed more severe systemic trabecular bone loss in a septic arthritis model. However, it remains unknown whether fracture-healing in osteoporotic bone is further delayed and if the level of infection is more severe in cases of FRI. The existing practice of antibiotic administration is to allow maintenance of implants, which has been shown to yield satisfactory results in 71% of cases.[15] However, it remains unclear if similar therapeutic effects of antibiotics can be achieved in osteoporotic bone with FRI.

Staphylococcus aureus is the most common pathogen for FRI.[16] When the fracture site is contaminated, planktonic bacteria cells form a matrix, and attach to an innate surface.[17] In addition, the colonization of the osteocyte-lacuno canalicular network (OLCN) has also been shown to be another major reservoir.[18] Typically, bacteria cells reside in biofilm in these locations and will undergo phenotype changes, including reduced division rate and metabolic activity, causing resistance to antibiotic treatment and phagocytosis of the host immune cells.[19] Current clinical recommendation is to retain the implant to allow for solid bone-healing, based on considerations of fixation stability, injury at FRI site, pathogens, and host comorbidities.[20] Early removal often leads to increased soft-tissue damage, dead space formation, and damage to revascularization, which are detrimental to both fracture-healing and control of infection.[7,20] The major difficulty for FRI treatment is therefore eradicating the biofilm formed on the implant, as well as the colony-forming units (CFUs) in the OLCN.[18,21] It remains unknown whether systemic antibiotics can effectively treat and promote healing in osteoporotic bone with FRI.[22]

This study aims to assess: 1) whether osteoporotic bone with FRI presents with more severe infection compared to normal bone with FRI; and 2) fracture healing and the effect of systemic antibiotics on pathogen clearance in both osteoporotic and normal bone with FRI.

Methods

Experimental design and induction of osteoporosis. With approval of the ethics committee (Ref: 18 to 140-OTC), 120 six-month-old Sprague Dawley (SD) rats were randomized into six groups: sham (Sham; n = 20); sham + infection (Sham-Inf; n = 20); sham + infection + antibiotic treatment (Sham-Inf-A; n = 20); ovariectomized (OVX; n = 20); ovariectomized + infection (OVX-Inf; n = 20); and ovariectomized + infection + antibiotic treatment (OVX-Inf-A; n = 20). Bilateral ovariectomy and sham surgery were performed according to our previously established protocols.[23] The rats were kept for three months with standard diet (catalogue number 50 IF/9 F, Picolab, USA) to develop osteoporosis, which was confirmed by bone mineral density (BMD) measurement with micro-CT. All rats underwent fracture surgery. We have included an ARRIVE checklist to show that we have conformed to the ARRIVE guidelines.

Establishment of fracture model. At nine months of age, all rats underwent diaphyseal fracture surgery at the femur shaft according to our established protocol.[23] In brief, the left knee joint was exposed with a medial parapatellar approach. The patella was dislocated, and femoral condyles were exposed. Following reaming with an 18-gauge needle, a 1.2 mm Kirschner wire (K-wire) was inserted through the intercondylar notch. The K-wire perforated through the proximal femur with the tip bent to prevent migration. The distal end was cut flush to allow movement of the knee joint. After closure, the fracture was made with a guillotine. Buprenorphine (0.1/100 g) was given before surgery and for three consecutive days after surgery to minimize pain.

Bacteria inoculation and antibiotic treatment. Following surgery, the fracture site was confirmed with radiographs.

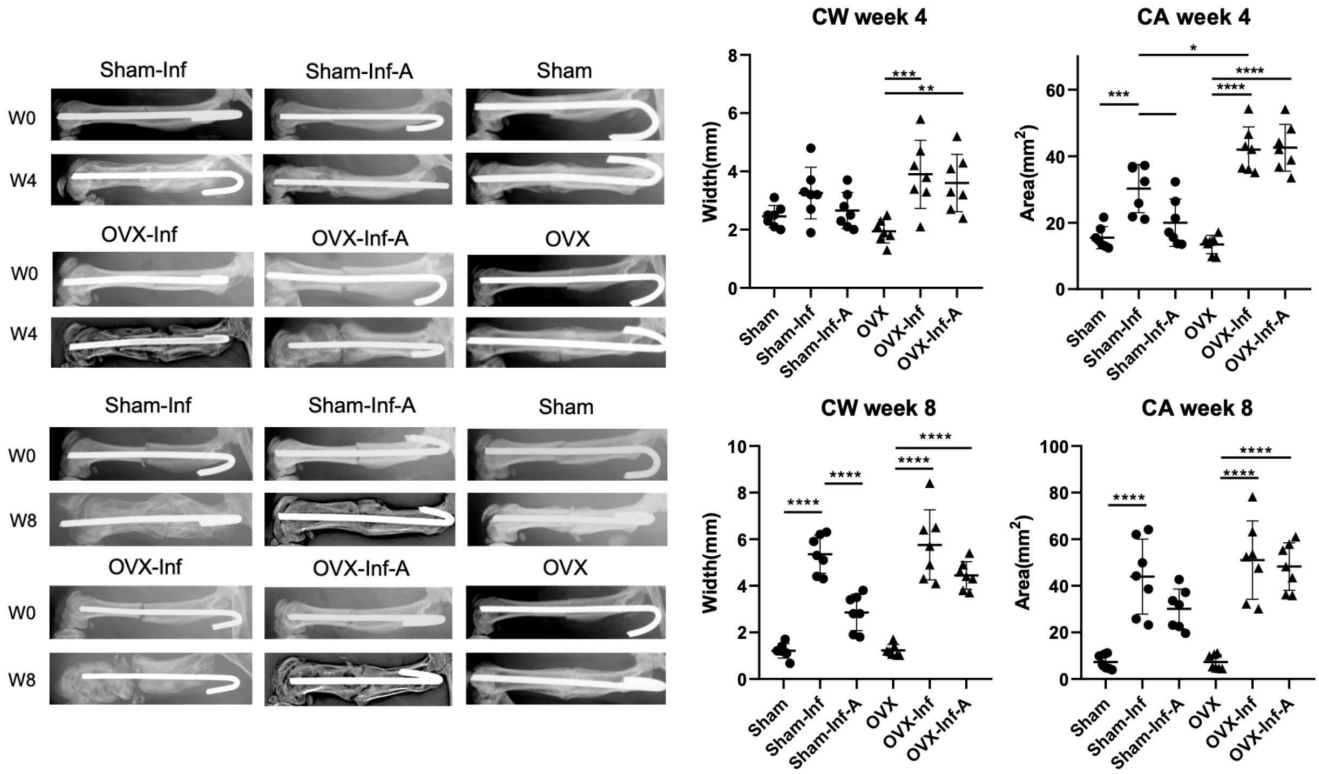

Fig. 1

Radiographs and quantitative analysis of callus width (CW) and callus area (CA) at week 4 and week 8 post-fracture. A, antibiotics; CA, callus area; CW, callus width; Inf, infection; OVX, ovariectomized. *p < 0.05; **p < 0.001; ***p < 0.001; ****p < 0.0001.

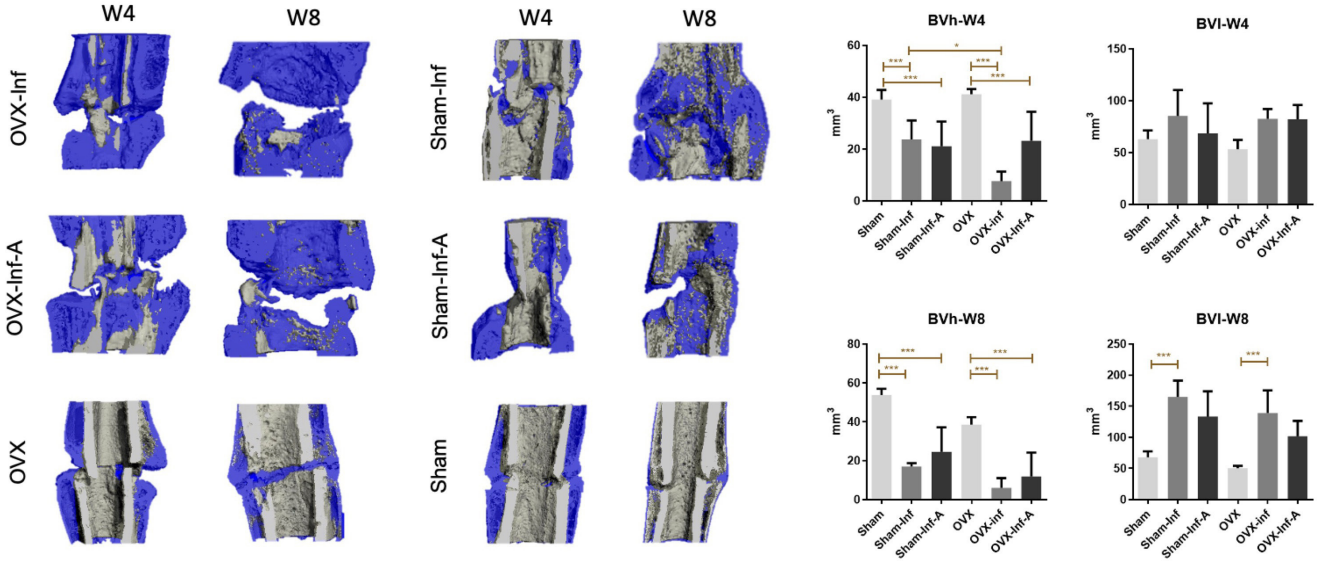

Fig. 2

Micro-CT analysis and quantitative analysis of high-density bone volume (BVh) and low-density bone volume (BVl) at week 4 and week 8. A, antibiotics; Inf, infection; OVX, ovariectomized. *p < 0.05; **p < 0.01; ***p < 0.001.

A 5 mm incision was made at the mid-femur shaft to approach the fracture site. The muscle and soft-tissue were separated, and the fracture site was exposed. Prepared bacteria suspension (*S. aureus ATCC25923*) at 10^4 CFU/ml was injected into the fracture site under direct vision. This strain is a clinical isolate with designation Seattle 1945, which is sensitive to methicillin. The wound was then sutured in layers. Rats in Sham-Inf-A and OVX-Inf-A were administered with Cefazolin (5 mg/kg).[24] Antibiotic treatment was applied daily, starting from 24 hours

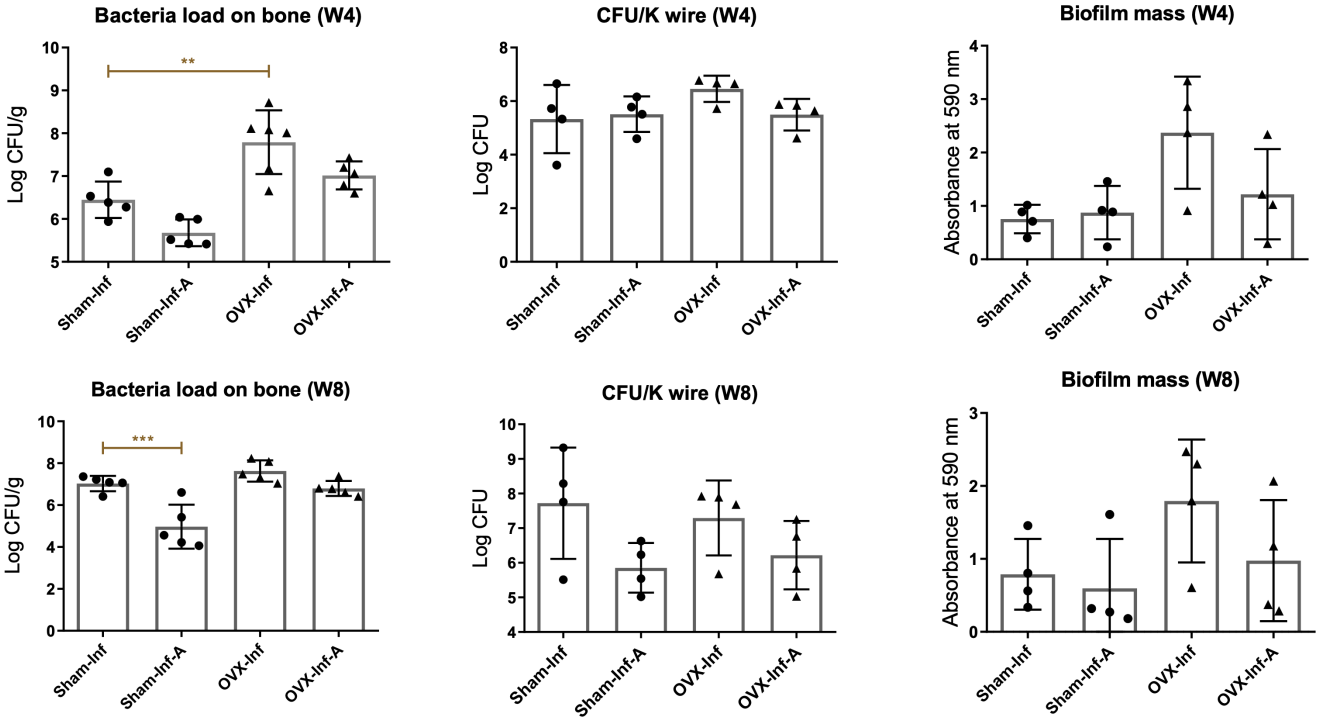

Fig. 3

Quantification of bacteria load on bone and Kirschner wire (K-wire) and biofilm mass on K-wire at week 4 and week 8. A, antibiotics; CFU, colony-forming unit; Inf, infection; OVX, ovariectomized. **p < 0.01; ***p < 0.001.

post-surgery to the endpoint at week 4 or week 8. The antibiotic treatment was applied to mimic the long-term application of systemic antibiotics in FRIs.[25]

Plain radiograph for fracture healing. Rats were killed at week 4 and week 8 post-surgery.[26] Anterior-posterior and lateral radiographs (Ultrafocus; Faxitron Bioptics LLC, USA) were obtained following initial operation and at euthanasia. Bone or joint destruction, bone sequestrum, cortical lysis, and periosteal thickening were observed. Quantification of callus morphology was performed with ImageJ software (National Institutes of Health, USA) according to our previous established protocol.[27] Callus width (CW) and callus area (CA) were measured.

Micro-CT analysis. After euthanasia, the femora were harvested and imaged with micro-CT (μCT-40, Scanco Medical, Switzerland). To observe changes in cortical bone and periosteal bone formation at the fracture site, the region of interest (ROI) was defined as 8.02 mm (422 slides) proximal and distal to the fracture according to our established protocol.[12] The volume of low-density bone (BVl, threshold = 165 to 350) and volume of high-density bone (BVh, threshold = 350 to 1,000) were reconstructed separately to differentiate newly formed bone and old cortical bone.[27]

CFU quantification in the bone tissue and K-wire. Following removal of K-wire, the entire bone sample was weighed and grinded. The suspension was diluted in a serial manner (1:1; 1:10; 1:100), and each dilution was streaked on agar plates and cultivated at 37°C for 24 hours. The number of CFU/g in bone was determined by the number of CFUs counted/initial weight of bone samples. The mean of all three dilutions was used to obtain the final number of CFU/g in bone.[28]

Bone histology. Bone samples were fixed with 10% neutral-buffered formalin and decalcified with 9% formic acid. Samples were processed, embedded in paraffin, and cut into 5 μm slices. Haematoxylin-eosin (H&E) staining was performed to observe histological signs of infection and bone-healing. A tissue quality score proposed by Shiels et al[29] was used to assess callus quality. In brief, callus quality was classified as 0: bony union; 1: most of the callus was new bone; 2: callus composed of new bone and spindle cells (major); 3: callus composed of inflammatory cells and spindle cells (major); and 4: most of the callus were inflammatory cells. An increasing score from 0 to 4 indicates decreased callus quality and further impaired healing. Modified gram staining, which targets the bacteria colonies in tissues with optimized contrast, was performed.[30] The number of CFUs embedded in the lacunae of cortical bone tissue was counted. Immunofluorescence was performed to confirm the presence of *S. aureus* in bone canals and OLCN. A primary antibody targeting the *S. aureus* protein A (1:500, ab20920; Abcam, UK) was used to identify the bacteria, and secondary antibody was red fluorescent (1:500, Alexa Fluor 594; Thermo Fisher Scientific, USA). Then, the slides were incubated with FITC (Fluorescein isothiocyanate isomer I, Sigma-Aldrich, USA), mounted with the Prolong Gold antifade reagent with DAPI (Thermo Fisher Scientific, USA), visualized under a confocal laser scanning microscopy

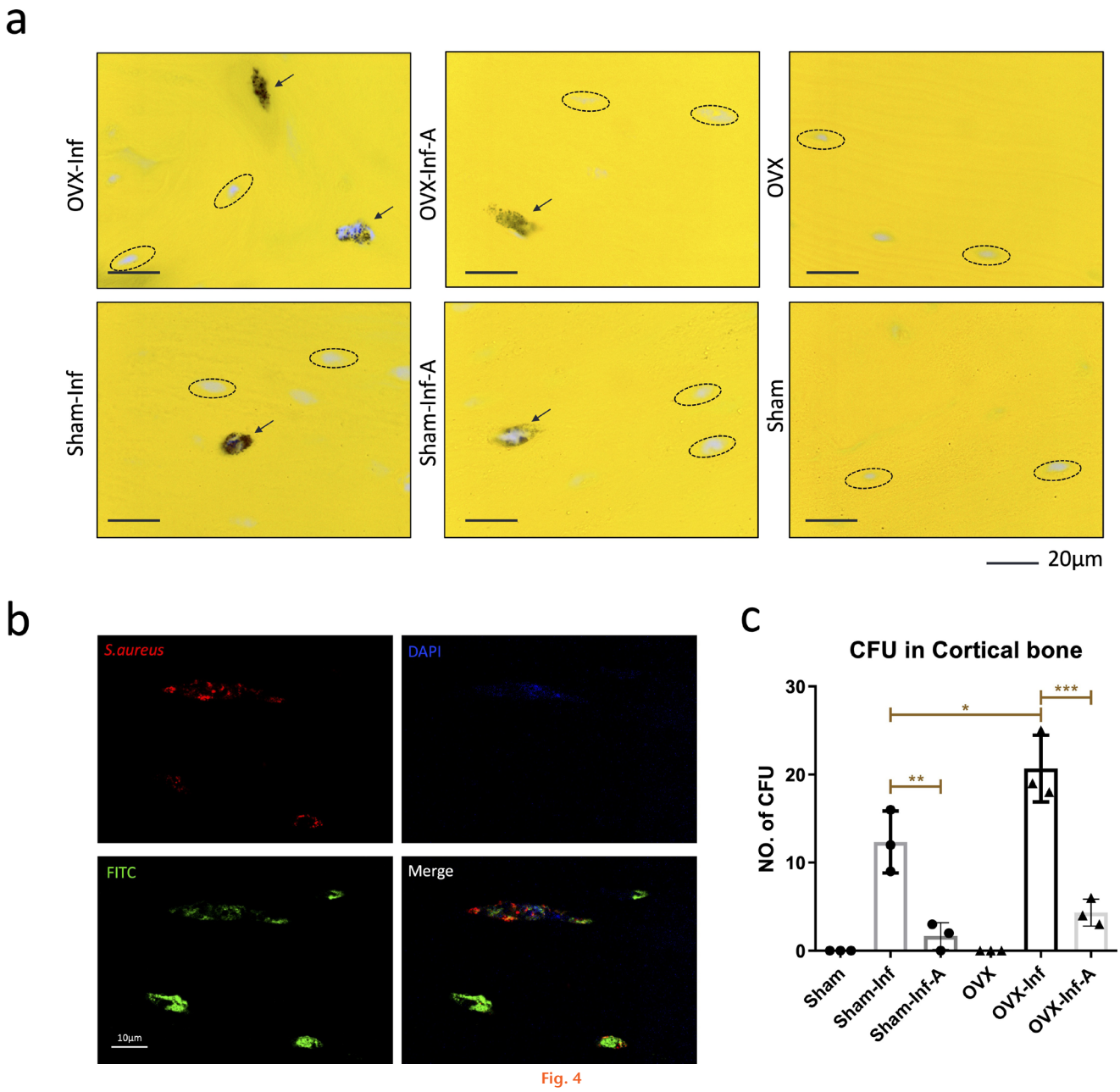

Fig. 4

a) As indicated by black arrows, Gram staining showed positively stained bacteria cells embedded in the ellipsoidal-shaped lacuna; b) the presence of bacteria in osteocyte-lacuno canalicular network was also confirmed with high resolution confocal laser scanning microscopy (1,000×); c) quantification of the bacteria colonization in the cortical bone tissue at week 4. A, antibiotics; CFU, colony-forming unit; DAPI, 4′,6-diamidino-2-phenylindole; FITC, fluorescein isothiocyanate isomer I; Inf, infection; OVX, ovariectomized; S. aureus, *Staphylococcus aureus*. *p < 0.05; **p < 0.01; ***p < 0.001.

(Zeiss, LSM 880, Germany) at 1,000× magnifications, and analyzed with ImageJ.

Inflammatory cytokines expression in serum and bone tissue. Enzyme-linked immunosorbent assay test was performed to quantify major inflammatory markers, including tumour necrosis factor alpha (TNF-α) and interleukin 6 (IL-6) concentrations in serum.[31] Expression of TNF-α in the bone tissue was determined by IHC staining. Following manufacturer's instruction for the Mouse and Rabbit Specific HRP/DAB IHC detection kit, the primary antibody for TNF-α (1:300, ab6671, Abcam) or negative control buffer were applied and incubated at 4°C overnight. Sections were counterstained with haematoxylin, and the positive expression of the protein at the targeted ROI at the fracture callus area was quantified by ImageJ software.

Bacterial load and biofilm mass on the K-wire. After euthanasia, the K-wire was removed in a sterile technique and sonicated in 3 ml phosphate-buffered saline (PBS; Thermo Fisher Scientific) to detach the biofilm.[32] The bacterial load on K-wire was determined by agar plating and CFU counting.[28] For the quantification of biofilm, it was

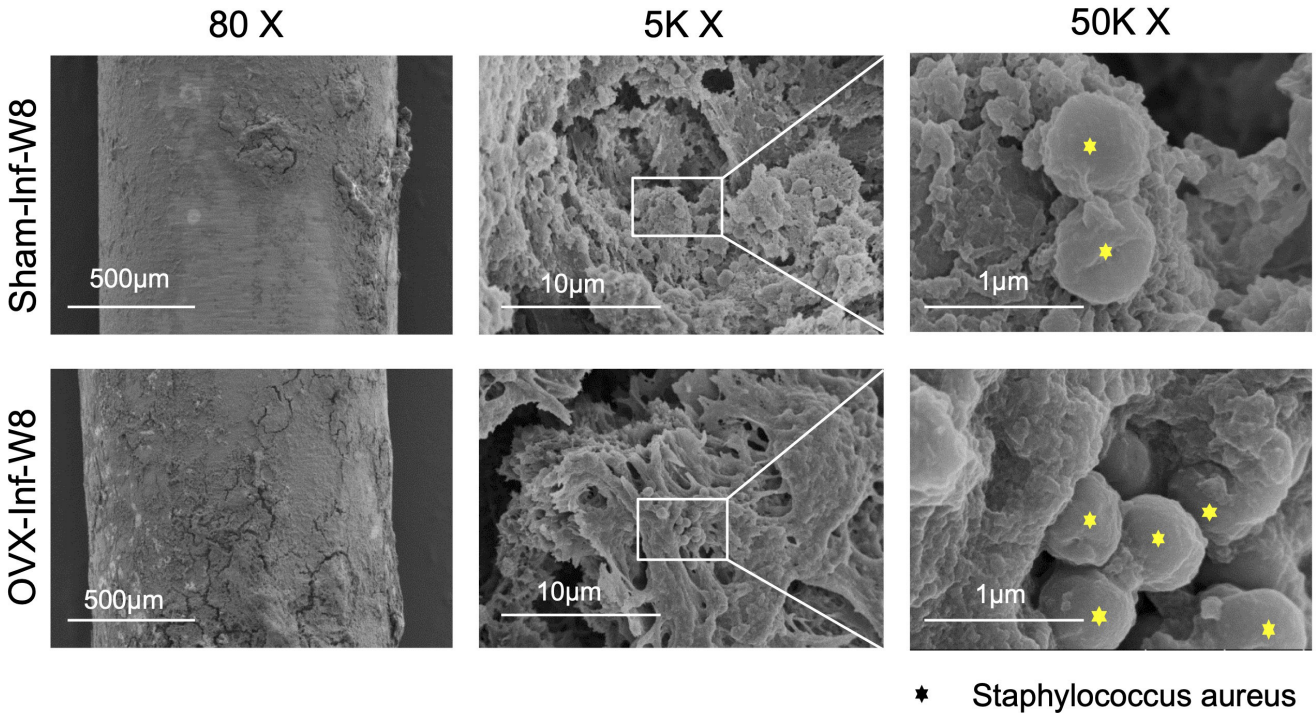

Fig. 5

Scanning electron microscopy imaging of biofilm formation on the Kirschner wire at week 8. OVX, ovariectomized; Sham-Inf-W8, sham with infection at week 8.

stained with 0.01% crystal violet (C0775; Sigma-Aldrich). Adherent crystal violet was solubilized in 33% glacial acetic acid (A6283; Sigma-Aldrich) and the optical density at 590 nm was determined by the microplate reader. The K-wire was cut into three pieces and processed with Glutaraldehyde solution, air-dried, mounted, sputter-coated with gold/palladium, and then assessed for biofilm formation by scanning electron microscopy (SEM).[28]

Mechanical testing. A four-point bending test was performed at eight weeks. Harvested femur was tested to failure with a constant displacement rate of 5 mm/min; load-displacement curves were generated. Parameters including the ultimate load (failure force) (N), stiffness (N/mm), and the energy to failure (N mm) were calculated with the QMAT Professional Material testing software (Tinius Olsen, UK).[33]

Statistical analysis. Statistical analysis was performed with SPSS v24.0 software (IBM, USA). All quantitative data were presented as mean and standard deviation (SD). Analysis of variance (ANOVA) and post-hoc Bonferroni test were used to compare the data at different timepoints. A p-value of ≤ 0.05 was considered statistically significant.

Results

All rats resumed weightbearing as tolerated post-surgery. Clinical signs of infection, including swelling and redness of the lower limbs, were observed in all rats with infection. Nine rats died whose cause of death included sepsis (n = 6) and severe wound purulent infection (n = 3). These rats were then replaced.

Radiological findings. At week 8, fracture healing rate was 91.6% in Sham (11/12), 8.3% in Sham-Inf (1/12), 66.7% in Sham-Inf-A (8/12), 91.6% in OVX (11/12), 0% in OVX-Inf, and 16.7% in OVX-Inf-A (2/12). At week 4, quantitative analysis showed a significantly higher callus area (CA) in OVX-Inf compared to Sham-Inf ($p = 0.013$). The callus width (CW) in OVX-Inf ($p < 0.001$) and OVX-Inf-A ($p = 0.006$) was significantly increased compared to OVX. In both OVX-Inf ($p < 0.001$) and OVX-Inf-A ($p < 0.001$), CA was significantly increased compared to OVX. In Sham-Inf, CA was significantly increased compared to Sham ($p < 0.001$) and Sham-Inf-A ($p = 0.046$). At week 8, for both OVX-Inf and OVX-Inf-A, CW and CA were significantly increased compared to OVX ($p < 0.001$). The CW in Sham-Inf was significantly increased compared to Sham ($p < 0.001$) and Sham-Inf-A ($p = 0.009$). Additionally, CA was significantly increased in Sham-Inf compared to Sham ($p < 0.001$). No other significant differences were observed (Figure 1). The comparison of CA and CW was made by ANOVA test and the p-values were generated with Bonferroni correction.

Micro-CT. At week 4, quantitative analysis showed a significantly lower volume of high-density bone (BVh) in OVX-Inf compared to Sham-Inf ($p = 0.023$). Moreover, BVh in OVX-Inf ($p < 0.001$) and OVX-Inf-A ($p = 0.030$) was significantly lower than that in OVX. The BVh in Sham-Inf ($p = 0.032$) and Sham-Inf-A ($p = 0.008$) was significantly higher than Sham. At week 8, BVh was significantly lower in OVX-Inf ($p < 0.001$) and OVX-Inf-A ($p < 0.001$) compared to OVX. BVh was significantly lower in

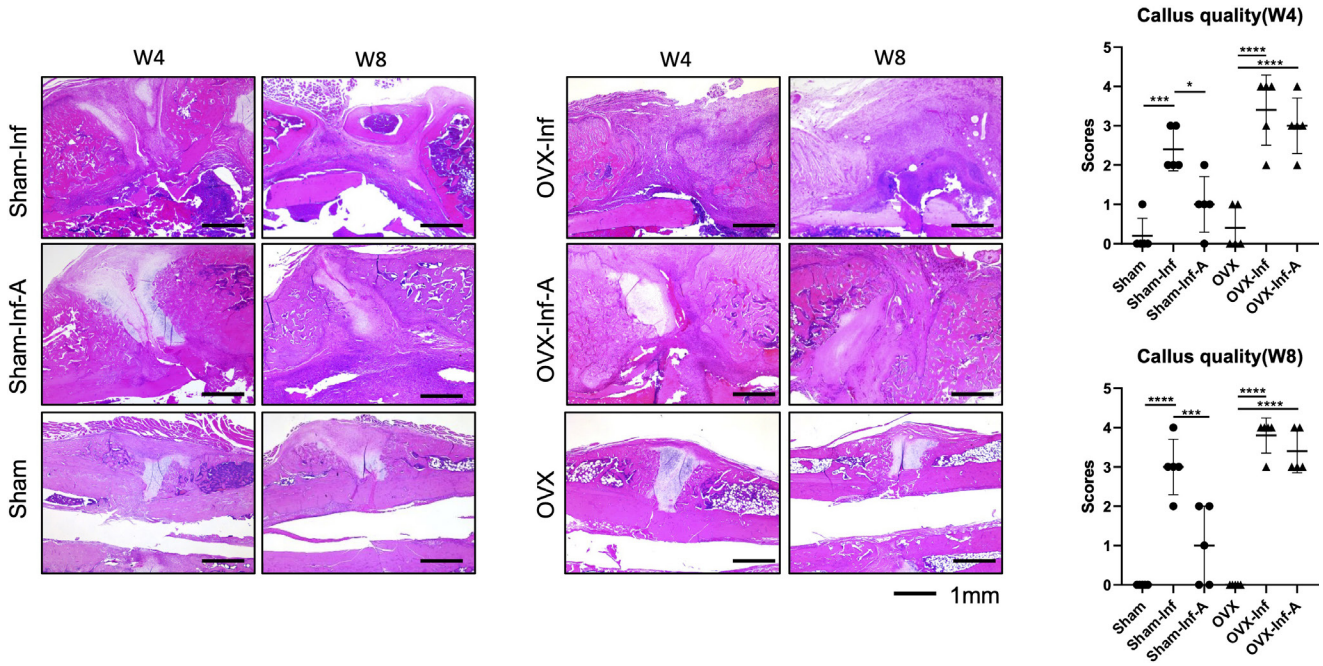

Fig. 6

Haematoxylin and eosin staining and quantification of callus quality at week 4 (W4) and week 8 (W8). A, antibiotics; Inf, infection; OVX, ovariectomized. *p < 0.05; **p < 0.01; ***p < 0.001; ****p < 0.0001.

Sham-Inf and Sham-Inf-A compared to Sham ($p < 0.001$). The volume of low-density bone (BVl) was significantly increased in Sham-Inf compared to Sham ($p < 0.001$), as well as OVX-Inf compared to OVX ($p < 0.001$) (Figure 2). The comparison of Bvh and Bvl was made by ANOVA test and p-values were generated with Bonferroni correction.

Bacterial load in bone. Agar plating showed that bacterial load in bone was significantly higher in OVX-Inf compared to Sham-Inf ($p = 0.002$) at week 4. At week 8, bacterial load in bone was significantly lower in Sham-Inf-A compared to Sham-Inf ($p < 0.001$) (Figure 3). Bacterial colonies were observed in the bone canals of the residual cortical bone (Figure 4a). Gram staining showed positively stained bacteria cells embedded in the ellipsoidal-shaped lacuna, which was arranged in parallel to the bone surface. These histological features indicate bacteria colonization in the OLCN.[34] The presence of bacteria in bone canals and OLCN was confirmed with high resolution confocal laser scanning microscopy (CLSM) (Figure 4b). Gram stain showed a significantly higher number of CFU embedded in the cortical bone in OVX-Inf compared to Sham-Inf at week 4 ($p = 0.039$) (Figure 4c).

SEM imaging, bacterial load, and the biofilm mass formation on K-wire. At week 8, bacteria biofilm was observed in all groups with infection. As shown in Figure 5, a large number of bacteria cells were found to be embedded in the polysaccharide matrix in both Sham-Inf and OVX-Inf by high-magnification SEM imaging. Agar plating showed no significant differences in bacterial load in bone among the four groups with infection for both weeks 4 and 8 (Figure 3). Similarly, for biofilm mass quantification by crystal violet (CV) staining, no significant difference was found.

Histological findings. The H&E staining and quantification is presented in Figure 6. Bone samples in all four groups with infection showed cortical thickening, inflammatory cell infiltration at the fracture site and bone marrow canal, and periosteal reaction. Despite no significant difference, the mean callus quality score was 2.4 (SD 0.6) in Sham-Inf, showing trend of higher callus quality than 3.4 (SD 0.9) in OVX-Inf at week 4. A similar trend was observed at week 8, with more severe inflammatory necrosis identified in OVX-Inf (Figure 6). Moreover, quantitative analysis showed a significantly enhanced callus quality ($p < 0.001$, ANOVA test with Bonferroni correction), as demonstrated by higher bony callus formation in Sham-Inf-A compared to Sham-Inf at week 8. In OVX-Inf-A, the fracture gap was found to be composed of spindle cells and inflammatory cells, with no bony callus. There was no significant improvement of callus quality in OVX-Inf-A compared to OVX-Inf.

Inflammatory cytokine expression in serum and fracture callus. The expression of serum inflammatory markers is presented in Figure 7. The comparison was made with ANOVA test and p-values were generated by Bonferroni correction. ELISA test showed a significant increase of IL-6 in OVX-Inf compared to OVX at week 4 ($p = 0.048$) and week 8 ($p = 0.0174$), and a significant increase of IL-6 in Sham-Inf compared to Sham ($p = 0.0397$) at week 8. At week 8, serum TNF-α was significantly increased in OVX-Inf compared to OVX ($p = 0.0281$). IHC staining showed a significantly higher expression of TNF-α expression at the

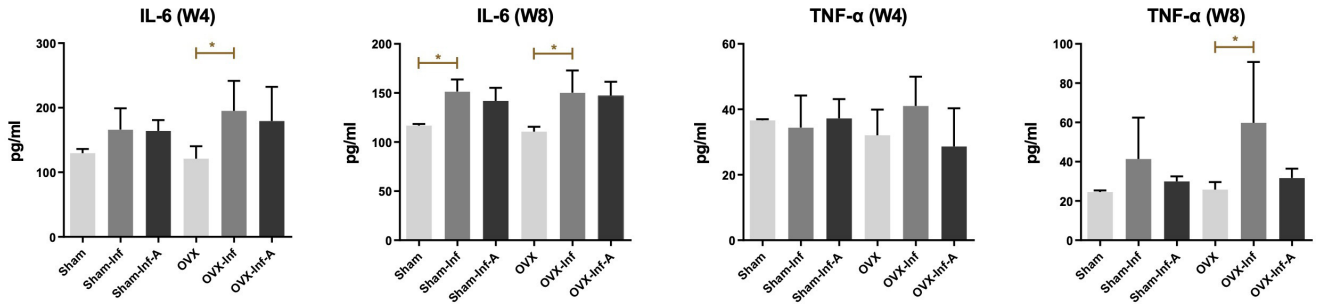

Fig. 7

Expression of serum inflammatory markers detected by enzyme-linked immunoassay test. A, antibiotics; IL, interleukin; Inf, infection; OVX, ovariectomized; TNF-α, tumour necrosis factor alpha; W, week. *p < 0.05.

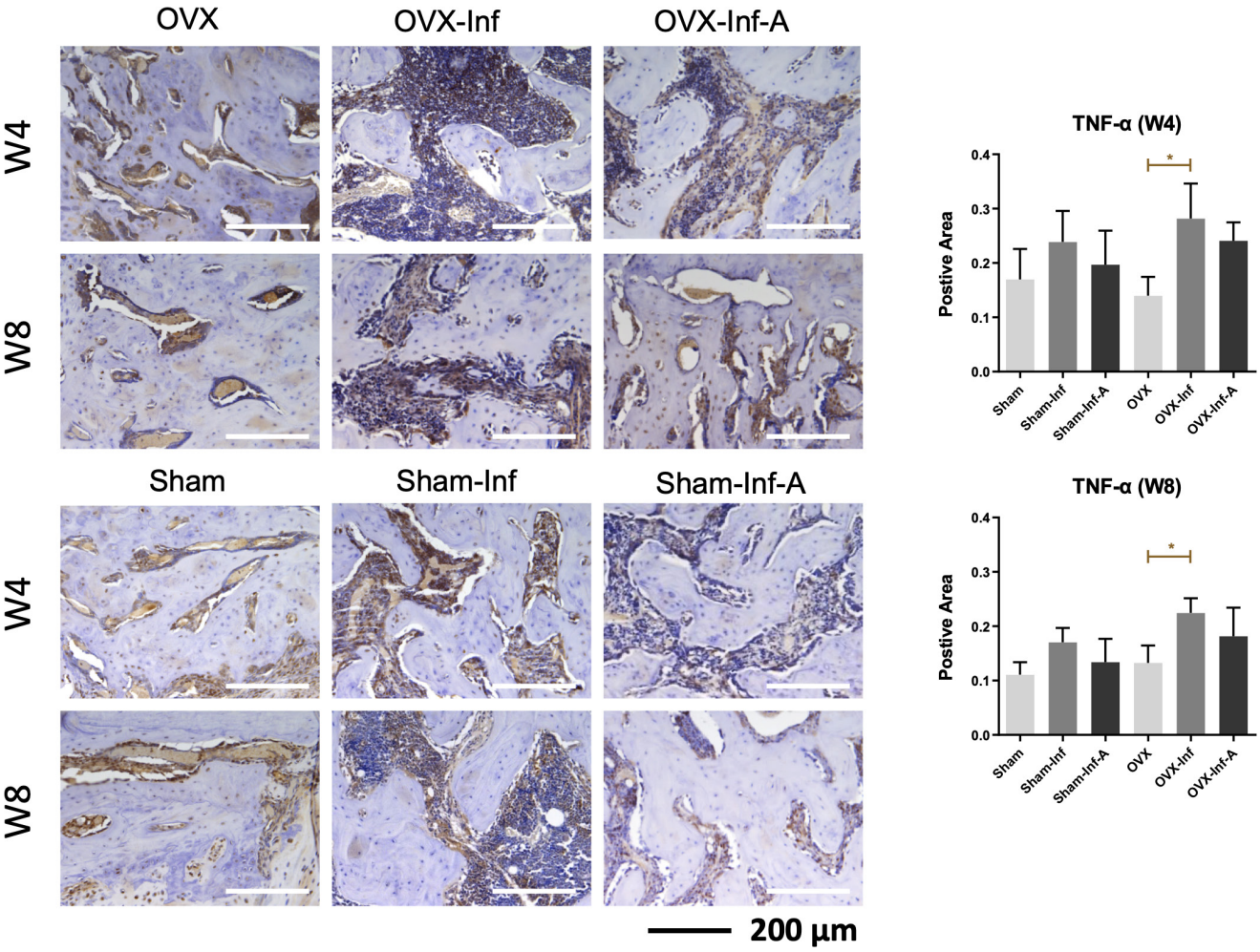

Fig. 8

Immunohistochemical staining of the tumour necrosis factor alpha (TNF-α) expression in fracture callus at week 4 (W4) and week 8 (W8). A, antibiotics; Inf, infection; OVX, ovariectomized. *p < 0.05.

fracture callus of OVX-Inf compared to OVX at both week 4 (p = 0.0490) and week 8 (p = 0.0334) (Figure 8).

Mechanical testing. Mechanical testing showed a significantly decreased ultimate load in Sham-Inf compared to Sham (p < 0.001), and increased ultimate load in Sham-Inf-A compared to Sham-Inf (p < 0.001). The ultimate load was decreased in both OVX-Inf (p < 0.001) and OVX-Inf-A (p = 0.001) compared to OVX. For stiffness, both Sham-Inf and OVX-Inf showed a significant decrease compared to Sham (p = 0.032) and OVX (p = 0.020), respectively. Similarly, both Sham-Inf and OVX-Inf showed a decreased energy to failure compared to Sham (p = 0.006) and OVX

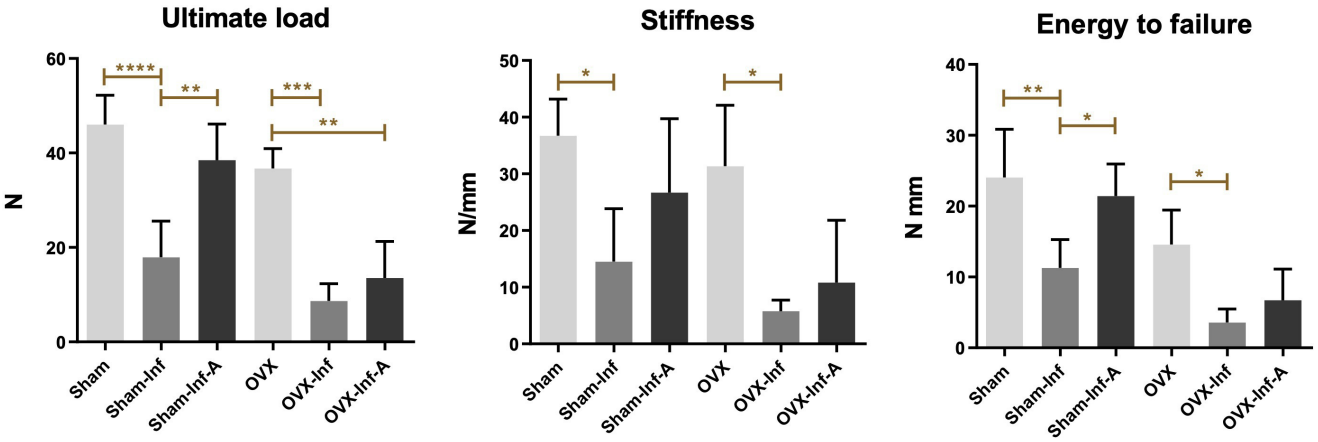

Fig. 9

Comparison of ultimate load, stiffness, and energy to failure in the mechanical test among six groups at week 8. A, antibiotics; Inf, infection; OVX, ovariectomized. *p < 0.05; **p < 0.01; ***p < 0.001; ****p < 0.0001.

(p = 0.046), respectively. In Sham-Inf-A, the energy to failure showed a significant increase compared to Sham-Inf (p = 0.028) (Figure 9). The comparison was made with ANOVA test and p-values were generated by Bonferroni correction.

Discussion

Fracture healing is delayed in osteoporotic bone,[23,35] or in the presence of wound contamination and FRI.[36-38] Mounting evidence has suggested sex differences in injury mechanism, pain, healing, and response to therapies, but the biological basis for this remains unclear.[39] Gjertsson et al[14] found that OVX induced more severe systemic bone loss in septic arthritis, which was attributed to the absence of oestrogen-induced serum interleukin production. However, it remains unknown if severity of infection and bone-healing is worse in osteoporotic bone with FRI. Clinically, the current consensus is to retain the implant if fixation is stable, as early implant removal will cause soft-tissue damage and worsening of infection.[21] One recent animal study also showed that instability leads to more pronounced local immune responses in a FRI model.[40] Despite the moderate effect of systemic antibiotic treatment on bacteria eradication and fracture-healing, its effect on FRI in osteoporosis also remains poorly understood. In the current study, we are the first group to identify further impaired healing in osteoporotic bone, which is evidenced by consistent changes including more drastic periosteal reaction, severe cortical bone lysis, and higher bacterial load and colonization on bone, as well as a trend towards uncontrolled inflammation and necrosis at the fracture site. More importantly, these changes were partially rescued in Sham-Inf by systemic antibiotic treatment, but not in OVX-Inf.

Cortical bone lysis and periosteal bone reaction are recognized as two key radiological features in acute bone infection.[22] Thompson et al[41] showed a similar pattern of BV loss and periosteal reaction in both OVX and Sham in a screw-related infection without fracture. However, BV loss between OVX-Inf and Sham-Inf were not compared in their study. In our study, significantly higher CW and lower BVh in the OVX-Inf were identified compared to Sham-Inf at week 4. These changes suggest a more robust periosteal bone reaction and cortical bone lysis in osteoporotic bone with FRI. Histologically, more severe inflammation and necrosis at the fracture site at week 8 also confirmed our findings on radiograph and micro-CT, suggesting a higher level of infection which further impaired callus remodelling.

The higher CFU number on bone samples indicated more severe infection in FRI with osteoporosis. In addition to bacterial contamination at the fracture site, colonization of the OLCN in the cortical bone tissue is another key pathological feature of FRI in chronic infection.[18] Bentley et al[18] labelled the bacteria colonies with BrdU and traced the *S. aureus* colonization through the canaliculi system by SEM in chronic osteomylites, which showed active migration of bacteria to cortical porosities. However, their observation was limited to the use of growing mice at eight to ten weeks of age, as cortical bone containing primary Harversian systems undergo multiple remodelling process. It remains unclear if cortical involvement still occurs in aged bone. In this study, we identified a higher CFU colonization in cortical bone tissue in osteoporotic bone with FRI. In addition to the fracture site, the cortical porosities serve as a natural reservoir for bacteria growth, which also protects them from phagocytosis by host immune cells.[18] Cortical porosity is a key feature of osteoporosis induced by OVX,[42] and this emerging evidence provided a possible explanation for our findings.

Biofilm formed on the K-wire in both OVX-Inf and Sham-Inf, which contributes to the formation of resistance to host immune response and antibiotic treatments.[43] In addition to the physiological barrier, bacteria colonies embedded in the biofilm also have phenotype changes, leading to an altered growth rate and nutrition consumption.[19] With these changes, the bacteria can survive a 1,000-fold dosage of the minimum

inhibitive concentration of antibiotics for planktonic bacteria. Although cefazolin is the first-line antibiotic for the treatment of FRI,[44] it has limited effects in shrinking the biofilm mass in both early and late stages, even if administered from day 0.[45] Similarly, cefazolin treatment in our study failed to significantly reduce the biofilm formation. Thus, future studies on a novel therapy targeting biofilm formation are warranted.

Significantly increased serum inflammatory cytokines in bone infection are well documented in one previous study.[31] We observed elevated serum IL-6 and TNF-α in both OVX-Inf and Sham-Inf. In a sterile fracture, a well-orchestrated local inflammatory response plays a vital role in callus formation and remodelling.[46] Our recent study demonstrated an impaired local inflammatory response in osteoporotic fracture callus, including decreased expression of TNF-α and IL-6 at week 1.[12] In the current study, significantly increased expression of TNF-α at week 4 and week 8 was identified in OVX-Inf compared to OVX. This prolonged elevation of TNF-α differs from normal inflammatory response at the early stage of healing. In infected bone tissue, the pathogen-associated molecular patterns (PAMPs) and Toll-like receptors (TLRs) expressed on multiple type of cells increases expression of multiple inflammatory cytokines including TNF, IL-1, and IL-6, leading to overactivation of osteoclast and bone lysis.[47] These changes, combined with higher bacterial load, lead to more severe periosteal reaction and bone loss, suggesting a further impaired response to FRI in osteoporotic bone.

Despite the well-accepted clinical principle of implant retention when the fixation is stable, complete eradication of infection is hardly achieved by systemic antibiotic treatment alone.[20,38] Shiels et al[48] identified that increasing the time to treat the open fracture would escalate the probability of biofilm maturation and diminish the effects of antibiotic-driven eradication. Our findings indicate that when started at 24 hours post-infection, an eight-week systemic cefazolin injection cannot eradicate the biofilm, but will reduce the planktonic bacteria, which is the phenotype that causes the immune response and subsequent poor healing.[31] Thompson et al[41] reported that OVX reduced antibiotic efficacy in a screw-related infection rat model. We have a similar observation of significantly reduced bacterial load in Sham-Inf at week 8, but not in OVX-Inf. Despite incomplete eradication of infection, antibiotic treatment was found to improve the callus remodelling histologically and augment its mechanical property in Sham-Inf. The disparity in infection resistance has also been noted in aggravated infection in the skin and knee joint induced by OVX.[14,49] In our study, the lower response to antibiotic treatment can be attributed to a high extent of cortical colonization, bone lysis, and disrupted local inflammatory response in osteoporotic bone. The CFUs in cortical porosities also have biofilm, which is difficult to penetrate by antibiotics.[50] Recently identified microRNA-186 and related morphogenetic protein (BMP) pathways provide a mechanistic understanding of bone-healing.[51] However, the mechanisms related to the disparities in immune response and antibiotic effectiveness in osteoporotic bone and normal bone remain to be defined in further studies. Given the immunoprotective effects of oestrogen in ameliorating bone loss in septic arthritis,[14] its potential effects on FRI also need to be further studied.

The strength of the current study is that we have elucidated further delayed healing in osteoporotic bone with FRI, radiologically and histologically. We also identified an increased bacterial load and more progressive colonization of OLCN in osteoporotic bone. The limitations are that only mono-antibiotic therapy was applied; further studies on other systemic antibiotics are required to examine its effect on fracture healing and bacterial load in FRI. Another limitation is that the molecular mechanisms have not yet been explored.

Our findings on the more severe infection and further delayed healing in osteoporotic bone with FRI revealed poor clinical outcomes and high rates of mortality. Given the biofilm formation on the implant, which cannot be eradicated by systemic antibiotic treatment in OVX-Inf-A, conventional treatment regimens including implant retention in elderly patients may need to be reviewed. Moreover, progressive colonization of OLCN also potentially challenges current debridement therapies by removing necrotic bone tissue only, which may largely fail to eradicate the colonization in the cortical bone. To address these problems, novel therapies targeting these key pathological changes are warranted to improve the outcomes and reduce the recurrence rate of FRI in osteoporotic bone. In addition to postmenopausal and senile osteoporosis, hormones, nutritional factors, and microbiota were suggested to regulate bone homeostasis and affect healing.[52,53] Smoking has also been shown to add to the risk of nonunion and infection in fracture treatment.[54,55] Future studies are needed to determine the potential hazardous effects of these factors on FRI, and provide insight into the risk management.[56]

In conclusion, the fracture-healing in osteoporotic bone with FRI was further delayed compared to normal bone, which was characterized by poorer callus remodelling, more severe periosteal reaction and bone lysis, and higher bacterial load on bone. In normal bone with FRI, systemic antibiotics were found to reduce bacterial load on bone, and improve callus quality and mechanical strength, but these effects were not observed in osteoporotic bone. More importantly, the more extensive cortical bone colonization in osteoporotic bone, which cannot be eradicated by systemic antibiotic treatment, suggested a possible mechanism for further impaired healing. These findings elucidated the lower success rate of implant retention and systemic antibiotic treatment in osteoporotic bone. To date, this is the first study that revealed the further impaired healing in osteoporotic bone with FRI. Given the increased risk of FRI in aged patients, the key pathological features revealed herein serve as the

therapeutic target for developing the future clinical treatment of osteoporotic bone with FRI.

Supplementary material

An ARRIVE checklist is included to show that the ARRIVE guidelines were adhered to in this study.

References

1. **Metsemakers WJ**, **Morgenstern M**, **McNally MA**, **et al**. Fracture-related infection: a consensus on definition from an international expert group. *Injury*. 2018;49(3):505–510.
2. **Court-Brown CM**, **Bugler KE**, **Clement ND**, **Duckworth AD**, **McQueen MM**. The epidemiology of open fractures in adults. A 15-year review. *Injury*. 2012;43(6):891–897.
3. **Wong RMY**, **Wong H**, **Zhang N**, **et al**. The relationship between sarcopenia and fragility fracture-a systematic review. *Osteoporos Int*. 2019;30(3):541–553.
4. **Wong RMY**, **Ho WT**, **Wai LS**, **et al**. Fragility fractures and imminent fracture risk in Hong Kong: one of the cities with longest life expectancies. *Arch Osteoporos*. 2019;14(1):104.
5. **Yano MH**, **Klautau GB**, **da Silva CB**, **et al**. Improved diagnosis of infection associated with osteosynthesis by use of sonication of fracture fixation implants. *J Clin Microbiol*. 2014;52(12):4176–4182.
6. **Metsemakers WJ**, **Morgenstern M**, **Senneville E**, **et al**. General treatment principles for fracture-related infection: recommendations from an international expert group. *Arch Orthop Trauma Surg*. 2020;140(8):1013–1027.
7. **Baertl S**, **Metsemakers WJ**, **Morgenstern M**, **et al**. Fracture-related infection. *Bone Joint Res*. 2021;10(6):351–353.
8. **Schwarz EM**, **Parvizi J**, **Gehrke T**, **et al**. 2018 International consensus meeting on musculoskeletal infection: research priorities from the general assembly questions. *J Orthop Res*. 2019;37(5):997–1006.
9. **Cheung WH**, **Miclau T**, **Chow S-H**, **Yang FF**, **Alt V**. Fracture healing in osteoporotic bone. *Injury*. 2016;47 Suppl 2:S21-6.
10. **Wong RMY**, **Li TK**, **Li J**, **et al**. A systematic review on current osteosynthesis-associated infection animal fracture models. *J Orthop Translat*. 2020;23:8–20.
11. **Wong RMY**, **Choy VMH**, **Li J**, **et al**. Fibrinolysis as a target to enhance osteoporotic fracture healing by vibration therapy in a metaphyseal fracture model. *Bone Joint Res*. 2021;10(1):41–50.
12. **Chow S-H**, **Chim Y-N**, **Wang J**, **et al**. Vibration treatment modulates macrophage polarisation and enhances early inflammatory response in oestrogen-deficient osteoporotic-fracture healing. *Eur Cell Mater*. 2019;38:228–245.
13. **Sakiani S**, **Olsen NJ**, **Kovacs WJ**. Gonadal steroids and humoral immunity. *Nat Rev Endocrinol*. 2013;9(1):56–62.
14. **Gjertsson I**, **Lagerquist MK**, **Kristiansson E**, **Carlsten H**, **Lindholm C**. Estradiol ameliorates arthritis and protects against systemic bone loss in Staphylococcus aureus infection in mice. *Arthritis Res Ther*. 2012;14(2):R76.
15. **Berkes M**, **Obremskey WT**, **Scannell B**, **et al**. Maintenance of hardware after early postoperative infection following fracture internal fixation. *J Bone Joint Surg Am*. 2010;92-A(4):823–828.
16. **Wong RMY**, **Li T-K**, **Li J**, **et al**. A systematic review on current osteosynthesis-associated infection animal fracture models. *J Orthop Translat*. 2020;23:8–20.
17. **Seebach E**, **Kubatzky KF**. Chronic implant-related bone infections-can immune modulation be a therapeutic strategy? *Front Immunol*. 2019;10:1724.
18. **de Mesy Bentley KL**, **Trombetta R**, **Nishitani K**, **et al**. Evidence of staphylococcus aureus deformation, proliferation, and migration in canaliculi of live cortical bone in murine models of osteomyelitis. *J Bone Miner Res*. 2017;32(5):985–990.
19. **Costerton JW**. Biofilm theory can guide the treatment of device-related orthopaedic infections. *Clin Orthop Relat Res*. 2005;(437):7–11.
20. **Morgenstern M**, **Kuehl R**, **Zalavras CG**, **et al**. The influence of duration of infection on outcome of debridement and implant retention in fracture-related infection. *Bone Joint J*. 2021;103-B(2):213–221.
21. **Gill SPS**, **Raj M**, **Singh P**, **Kumar D**, **Singh J**, **Rastogi P**. Infected nonunion with implant in situ in long bone fractures, managed by retention of implant-our experience. *J Orthop Traumatol Rehabil*. 2017;9(1):29.
22. **Croes M**, **van der Wal BCH**, **Vogely HC**. Impact of bacterial infections on osteogenesis: evidence from in vivo studies. *J Orthop Res*. 2019;37(10):2067–2076.
23. **Wong RM**, **Thormann U**, **Choy MH**, **et al**. A metaphyseal fracture rat model for mechanistic studies of osteoporotic bone healing. *Eur Cell Mater*. 2019;37:420–430.
24. **Penn-Barwell JG**, **Murray CK**, **Wenke JC**. Early antibiotics and debridement independently reduce infection in an open fracture model. *J Bone Joint Surg Br*. 2012;94-B(1):107–112.
25. **Fang C**, **Wong T-M**, **To KK**, **Wong SS**, **Lau T-W**, **Leung F**. Infection after fracture osteosynthesis - Part II. *J Orthop Surg*. 2017;25(1):2309499017692714.
26. **Alt V**, **Thormann U**, **Ray S**, **et al**. A new metaphyseal bone defect model in osteoporotic rats to study biomaterials for the enhancement of bone healing in osteoporotic fractures. *Acta Biomater*. 2013;9(6):7035–7042.
27. **Cheung WH**, **Chin WC**, **Qin L**, **Leung KS**. Low intensity pulsed ultrasound enhances fracture healing in both ovariectomy-induced osteoporotic and age-matched normal bones. *J Orthop Res*. 2012;30(1):129–136.
28. **Alt V**, **Lips KS**, **Henkenbehrens C**, **et al**. A new animal model for implant-related infected non-unions after intramedullary fixation of the tibia in rats with fluorescent in situ hybridization of bacteria in bone infection. *Bone*. 2011;48(5):1146–1153.
29. **Shiels SM**, **Bouchard M**, **Wang H**, **Wenke JC**. Chlorhexidine-releasing implant coating on intramedullary nail reduces infection in a rat model. *Eur Cell Mater*. 2018;35:178–194.
30. **Becerra SC**, **Roy DC**, **Sanchez CJ**, **Christy RJ**, **Burmeister DM**. An optimized staining technique for the detection of Gram positive and Gram negative bacteria within tissue. *BMC Res Notes*. 2016;9(1):1–10.
31. **Lüthje FL**, **Jensen LK**, **Jensen HE**, **Skovgaard K**. The inflammatory response to bone infection - a review based on animal models and human patients. *APMIS*. 2020;128(4):275–286.
32. **Bjerkan G**, **Witsø E**, **Bergh K**. Sonication is superior to scraping for retrieval of bacteria in biofilm on titanium and steel surfaces in vitro. *Acta Orthop*. 2009;80(2):245–250.
33. **Shi H-F**, **Cheung W-H**, **Qin L**, **Leung A-C**, **Leung K-S**. Low-magnitude high-frequency vibration treatment augments fracture healing in ovariectomy-induced osteoporotic bone. *Bone*. 2010;46(5):1299–1305.
34. **Shah FA**, **Zanghellini E**, **Matic A**, **Thomsen P**, **Palmquist A**. The orientation of nanoscale apatite platelets in relation to osteoblastic-osteocyte lacunae on trabecular bone surface. *Calcif Tissue Int*. 2016;98(2):193–205.
35. **Choy M-H**, **Wong R-Y**, **Li M-C**, **et al**. Can we enhance osteoporotic metaphyseal fracture healing through enhancing ultrastructural and functional changes of osteocytes in cortical bone with low-magnitude high-frequency vibration? *FASEB J*. 2020;34(3):4234–4252.
36. **Cole HA**, **Ohba T**, **Nyman JS**, **et al**. Fibrin accumulation secondary to loss of plasmin-mediated fibrinolysis drives inflammatory osteoporosis in mice. *Arthritis Rheumatol*. 2014;66(8):2222–2233.
37. **Bilgili F**, **Balci HI**, **Karaytug K**, **et al**. Can normal fracture healing be achieved when the implant is retained on the basis of infection? an experimental animal model. *Clin Orthop Relat Res*. 2015;473(10):3190–3196.
38. **Foster AL**, **Moriarty TF**, **Zalavras C**, **et al**. The influence of biomechanical stability on bone healing and fracture-related infection: the legacy of Stephan Perren. *Injury*. 2021;52(1):43–52.
39. **Clarke SA**. The inadequate reporting of sex in research: applying the lessons from COVID-19 to speed up the availability of sex-based data. *Bone Joint Res*. 2020;9(10):729–773.
40. **Sabaté-Brescó M**, **Berset CM**, **Zeiter S**, **et al**. Fracture biomechanics influence local and systemic immune responses in a murine fracture-related infection model. *Biol Open*. 2021;10(9):bio057315.
41. **Thompson K**, **Freitag L**, **Styger U**, **et al**. Impact of low bone mass and antiresorptive therapy on antibiotic efficacy in a rat model of orthopedic device-related infection. *J Orthop Res*. 2021;39(2):415–425.
42. **Harrison KD**, **Hiebert BD**, **Panahifar A**, **et al**. Cortical Bone Porosity in Rabbit Models of Osteoporosis. *J Bone Miner Res*. 2020;35(11):2211–2228.
43. **Masters EA**, **Trombetta RP**, **de Mesy Bentley KL**, **et al**. Evolving concepts in bone infection: redefining "biofilm", "acute vs. chronic osteomyelitis", "the immune proteome" and "local antibiotic therapy". *Bone Res*. 2019;7:20.
44. **Redfern J**, **Wasilko SM**, **Groth ME**, **McMillian WD**, **Bartlett CS 3rd**. Surgical site infections in patients with type 3 open fractures: comparing antibiotic prophylaxis with cefazolin plus gentamicin versus piperacillin/tazobactam. *J Orthop Trauma*. 2016;30(8):415–419.
45. **Tomizawa T**, **Nishitani K**, **Ito H**, **et al**. The limitations of mono- and combination antibiotic therapies on immature biofilms in a murine model of implant-associated osteomyelitis. *J Orthop Res*. 2021;39(2):449–457.
46. **Chow S-H**, **Chim Y-N**, **Wang J-Y**, **Wong R-Y**, **Choy V-H**, **Cheung W-H**. Inflammatory response in postmenopausal osteoporotic fracture healing. *Bone Joint Res*. 2020;9(7):368–385.

47. **Nishitani K**, **Bello-Irizarry SN**, **de Mesy Bentley KL**, **Daiss JL**, **Schwarz EM**. Chapter 16 - The Role of the Immune System and Bone Cells in Acute and Chronic Osteomyelitis. In: Lorenzo J, Horowitz MC, Choi Y, Takayanagi H, Schett G, eds. *Osteoimmunology: Interactions of the Immune and Skeletal Systems*. Second ed. Cambridge, Massachusetts: Academic Press, 2015: 283–295.
48. **Shiels SM**, **Tennent DJ**, **Lofgren AL**, **Wenke JC**. Topical rifampin powder for orthopaedic trauma part II: topical rifampin allows for spontaneous bone healing in sterile and contaminated wounds. *J Orthop Res*. 2018;36(12):3142–3150.
49. **Castleman MJ**, **Pokhrel S**, **Triplett KD**, **et al**. Innate sex bias of staphylococcus aureus skin infection is driven by α-hemolysin. *J Immunol*. 2018;200(2):657–668.
50. **Nishitani K**, **Sutipornpalangkul W**, **de Mesy Bentley KL**, **et al**. Quantifying the natural history of biofilm formation in vivo during the establishment of chronic implant-associated Staphylococcus aureus osteomyelitis in mice to identify critical pathogen and host factors. *J Orthop Res*. 2015;33(9):1311–1319.
51. **Wang C**, **Zheng G-F**, **Xu X-F**. MicroRNA-186 improves fracture healing through activating the bone morphogenetic protein signalling pathway by inhibiting SMAD6 in a mouse model of femoral fracture: an animal study. *Bone Joint Res*. 2019;8(11):550–562.
52. **Li J**, **Ho WTP**, **Liu C**, **et al**. The role of gut microbiota in bone homeostasis: a systematic review of preclinical animal studies. *Bone Joint Res*. 2021;10(1):51–59.
53. **Li S**, **Mao Y**, **Zhou F**, **Yang H**, **Shi Q**, **Meng B**. Gut microbiome and osteoporosis: a review. *Bone Joint Res*. 2020;9(8):524–530.
54. **Hernigou J**, **Schuind F**. Tobacco and bone fractures: a review of the facts and issues that every orthopaedic surgeon should know. *Bone Joint Res*. 2019;8(6):255–265.
55. **Chang C-J**, **Jou I-M**, **Wu T-T**, **Su F-C**, **Tai T-W**. Cigarette smoke inhalation impairs angiogenesis in early bone healing processes and delays fracture union. *Bone Joint Res*. 2020;9(3):99–107.
56. **Nicholson T**, **Scott A**, **Newton Ede M**, **Jones SW**. Do E-cigarettes and vaping have a lower risk of osteoporosis, nonunion, and infection than tobacco smoking? *Bone Joint Res*. 2021;10(3):188–191.

Author information:
- J. Li, MMed, PhD Student
- R. M. Y. Wong, MBChB, FRCSEd (Orth), PhD, Clinical Assistant Professor
- Y. L. Chung, BSc, Research Assistant
- S. K-H. Chow, PhD, Research Assistant Professor
- W-H. Cheung, PhD, Professor
  Department of Orthopaedics & Traumatology, The Chinese University of Hong Kong, Hong Kong, China.
- S. S. Y. Leung, BEng (Chemical Eng) (Hons), PhD, Assistant Professor, School of Pharmacy, The Chinese University of Hong Kong, Hong Kong, China.
- M. Ip, FRCPath, FRCP(Glasg), FRCPA, Professor, Department of Microbiology, Prince of Wales Hospital, The Chinese University of Hong Kong, Hong Kong, China.

Author contributions:
- J. Li: Investigation, Formal analysis, Writing – original draft.
- R. M. Y. Wong: Conceptualization, Formal analysis, Writing – original draft, Supervision.
- Y. L. Chung: Investigation.
- S. Leung Shi Yee : Conceptualization, Writing – review & editing.
- S. K-H. Chow: Conceptualization, Writing – review & editing.
- M. Ip: Conceptualization, Writing – review & editing, Supervision.
- W-H. Cheung: Conceptualization, Writing – review & editing, Supervision.

- J. Li and R. M. Y. Wong are joint first authors.

- M. Ip and W-H. Cheung are joint senior authors.

Funding statement:
- The author(s) disclose receipt of the following financial or material support for the research, authorship, and/or publication of this article: the OTC grant (Ref: 2018-RWMI), CUHK Direct Grant for Research (Ref: 2018.062), and CUHK Direct Grant for Research (Ref: 2019.058).

ICMJE COI statement:
- S. Leung Shui Yee reports funding from the Health and Medical Research Fund (Ref: 19180062), unrelated to this study.

Data sharing:
- The study protocol was prepared before the study. The key data of the study were presented with the figures enclosed.

Open access funding
- The authors confirm that the open access fee for this study was provided by the OTC grant (Ref: 2018-RWMI).